ICARUS 100, 288–294 (1992)

Physical Observations of (5145) Pholus

MARC W. BUIE AND SCHELTE J. BUS

Lowell Observatory, 1400 West Mars Hill Road, Flagstaff, Arizona 86001

Received July 31, 1992; revised September 25, 1992

We present physical measurements of the newly discovered asteroid, (5145) Pholus, based on seven nights of photometric observations. These observations determine an unambiguous lightcurve period of 9.9825 ± 0.0040 hr with a peak-to-peak amplitude of 0.15 mag. We also report a rotationally independent color of $(V - R) = 0.810 \pm 0.006$ (Kron–Cousins R). The standard IAU two parameter fit versus solar phase angle yields $H_V = 7.645 \pm 0.011$ and $G_V = 0.16 \pm 0.08$. Except for its color and orbit, (5145) Pholus exhibits normal asteroidal properties.

INTRODUCTION

A distant Solar System object was discovered on UT 1992 January 9 by Rabinowitz as part of the Spacewatch Program (Scotti 1992). Asteroidal in appearance, this object was given the preliminary designation of 1992 AD. Subsequent astrometry along with prediscovery observations by Shoemaker from UT 1992 January 1 led to the orbit by Williams (1992a) showing 1992 AD to be in a Chiron-like orbit with an orbital period of 93 years and a perihelion distance just inside the orbit of Saturn. On the basis of additional prediscovery observations, Williams (1992b) determined a secure orbit leading to the assignment of the minor planet number of 5145 and the name Pholus (from MPC 20523).

Unlike (2060) Chiron, discovered far from its perihelion distance of 8.5 AU, (5145) Pholus had just passed perihelion at discovery. This geometry provides observers the best opportunity to obtain physical observations and especially to search for any evidence of cometary activity similar to (2060) Chiron. Howell *et al.* (1992) obtained the first thermal detection of (5145) Pholus at both 10.6 and 21 μm and provided a standard thermal model estimate for the diameter of 140 km with a geometric albedo of 0.08. However, this estimate should be regarded as a lower limit on the size as suggested by Spencer *et al.* (1989). Depending on the subsolar latitude at the time of observations, the actual albedo could be as low as a few percent.

Hainaut and Smette (1992) reported a search for cometary activity but they found no evidence of an extended coma in direct images and the spectrum was similar to that of the Sun in appearance with no cometary emission lines. We published a preliminary lightcurve period of 9.996 ± 0.030 hr with an amplitude of 0.17 mag (Buie *et al.* 1992). Soon after, Hoffman *et al.* (1992) published a period of 0.55 days (13.2 hr) based on CCD photometry which they obtained on 30 and 31 January 1992 UT. We suggest that the period they derived is a 4 : 3 alias of the true period. This alias is present in our more extensive set of observations but is clearly not the true period.

Immediately after discovery, Mueller and Tholen (Mueller *et al.* 1992) independently realized that (5145) Pholus was redder in color than any other asteroid or comet previously observed. A visible spectrum obtained by Fink *et al.* (1992) and *JHK* photometry reported by Davies and Sykes (1992) also reflect the steep red color. Fink *et al.* (1992) attribute the color to the presence of tholins on the surface. Tholins are the result of long-term exposure of organic molecules to energetic radiation (Khare *et al.* 1981) and would thus imply a carbon-bearing volatile reservoir on or near the surface. Mueller *et al.* (1992) also suggest tholins but also discuss ion-irradiated methane ice (Strazzulla *et al.* 1984) as a possible surface constituent.

This red slope is in sharp contrast to the nearly neutral color of (2060) Chiron. While the unstable nature of Chiron's present orbit has been well documented (e.g., Kowal *et al.* 1979, Oikawa and Everhart 1979, Scholl 1979, Hahn and Bailey 1990), no such studies exist yet for the long-term orbital evolution of (5145) Pholus. However, close approaches to Saturn may greatly influence this object's orbit over short timescales (Mueller *et al.* 1992). Thus, the question of origin of (5145) Pholus and similarly that of Chiron is difficult to address. If this object is a freak escapee from the main belt, the unique color of (5145) Pholus would define a new asteroid spectral class with no other known members (Z-type as suggested by Mueller *et al.* 1992). If Chiron and (5145) Pholus were both derived

0019-1035/92 $5.00

TABLE I
Summary of Observations

UT Date	Time	r	Δ	α	Filter	N	Conditions
1992 Jan 25	5:50-12:11	8.703	7.722	0.60	V	6	photometric
1992 Jan 26	5:52-12:19	8.703	7.724	0.73	R	23	variable clouds
1992 Feb 01	5:00-11:54	8.705	7.742	1.46	R	72	nearly photometric
1992 Feb 05	2:31-11:42	8.706	7.760	1.94	R*	41	variable clouds
1992 Feb 22	2:29-07:37	8.712	7.887	3.78	V,R	12,43	variable clouds
1992 Feb 23	3:32-08:41	8.712	7.898	3.88	R	36	variable clouds
1992 Feb 24	2:19-09:16	8.712	7.907	3.97	V,R	20,27	photometric

recently from the inner Oort Cloud, the difference in their respective colors may be due entirely to Chiron's current cometary activity and the apparent lack of activity on (5145) Pholus.

Our goal in obtaining the CCD photometry for this project was to compare the lightcurve and photometric phase curve for (5145) Pholus with other asteroids and comets. We were also looking for variations in the $(V - R)$ color as a function of rotation.

OBSERVATIONS AND REDUCTIONS

A summary of observations appears in Table I. Each row corresponds to a single night of observations on (5145) Pholus for the time span listed. For each night, we provide the mean asteroid–Sun distance r in AU, the mean asteroid–Earth distance Δ in AU, and the mean solar phase angle. We also list the filters used during the night, the number of measurements taken with each filter, and a general comment on the quality of the night. All observations were made by S. J. Bus with additional help from B. A. Skiff on 1992 February 01 and from M. W. Buie on 1992 February 22–24.

The observations on the night of UT 1992 February 05 were taken at the Perkins 1.8-m telescope on Anderson Mesa. We used the NSF-TI 800 × 800 CCD mounted on the OSU imaging Fabry–Perot spectrograph configured as a 5 : 1 focal reducing camera. This setup gave a nominal image scale of 0.48 arcsec per pixel. The filter we used approximated an R filter with a central wavelength of 7009 Å and a FWHM of 2601 Å.

All other observations were taken at the John S. Hall 1.1-m telescope on Anderson Mesa using an RCA 320 × 512 CCD. All of these observations were done with the $f/8$ secondary and no focal reducer, giving a nominal image scale of 0.7 arcsec per pixel. We took both V and R data with this setup. The R filter we used provides a good match to the Kron–Cousins R system. The V filter is a somewhat poorer match to Johnson V with a central wavelength of 5518 Å and a FWHM of 1196 Å but is asymmetric to the red end of the filter.

The processing of all CCD frames followed standard procedures. The NSF-TI data were bias corrected from the overscan region and then flattened with averaged dome flats. Processing the RCA CCD data required one additional step of creating an average bias frame and then subtracting this frame, pixel by pixel, from each object frame before dividing by the flat field. For 1.1-m data we used a dome flat for the V filter and a twilight sky flat for the R filter.

The extraction of an instrumental photometric magnitude from each CCD frame was done with a IRAF-compatible program named "basphotc" written by M. W. Buie and ported to IRAF by Frank Valdes at NOAO. This program is available for general use and can be obtained by contacting Buie. Basphotc allows for the interactive measurement of the location and brightness of any source using circular apertures for both the object and the sky signal. There is an additional mode primarily intended for comet photometry that allows the interactive selection of sky regions that are free of field stars or signal from the program object itself.

Coarse positioning of the photometric aperture is done via an interactive cursor on the workstation image display. From the coarse position, the brightest nearby pixel is recorded. The bright pixel search occurs over a square region whose width is the same as the diameter of the object aperture. Next, the center of light of the object aperture is computed without subtracting any sky signal using the brightest pixel as the center of the aperture. The nonintegral pixel location of the approximate center of light is then used as the location for the final photometric aperture. As a final check, a new center of light is computed for the sky subtracted object aperture. If the data are well behaved, the two center-of-light measurements will be very close. Small object apertures used for on-chip differential photometry require this consistent approach to aperture centering. Failure to accurately center the aperture on the object will increase the noise in the extracted photometry.

To integrate the signal within the object aperture, we perform a weighted sum of the intensity of all pixels that are included within our aperture either in whole or in part. The weight for each pixel in the summation is the fraction of its area which is included within the aperture. This weight is computed analytically and is exact. We make no provision within this summation for pixels contaminated by field stars, cosmic ray strikes, or bad pixels. We discard any measurements that are contaminated in these ways, but in practice we discarded very few.

The computation of the sky signal is more intricate. From the inner and outer radii of the sky annulus, all pixels are extracted whose centers are within the annulus. The sky signal and its uncertainty are determined from a robust mean of this sample. This computation begins by computing the first four statistical moments of the sky sample (mean, variance, skew, and kurtosis) and their uncertainties. If the skew and kurtosis are not representa-

tive of a normal distribution, any sky pixels that differ from the sky mean by more than 5 σ are removed from the sample. If some points are removed, the process is repeated until either no outliers exist or the variance converges and the skew and kurtosis take on reasonable values for a normal distribution. A very good discussion of skew and kurtosis and their uncertainties can be found in Press *et al.* (1988).

This complicated strategy works extremely well in measuring the sky background as long as the sky annulus is large. For this dataset, all measurements were made with an annulus having a 10-pixel inner radius and a 50-pixel outer radius. Cosmic ray strikes, bad pixels, and field stars are all automatically excluded from the sky sample, making the placement of the photometric aperture trivial. Tests with manually placed sky apertures that are known to exclude outlier pixels always achieve the same answer as the automatic routine.

An equally important step is the computation of the uncertainties for each instrumental magnitude. The uncertainty of the background is just the standard deviation of the sky pixels left after removing the outliers. This uncertainty automatically includes scatter caused by photon noise from the sky, flat fielding noise, and CCD readout noise. The uncertainty for the object is computed assuming that photon counting noise dominates the object signal above background. We have found that the uncertainties are reliable as long as the gain of the system is known and the flat fielding correction is not too large.

Except for the 1992 January 25 data, we measured the asteroid differentially with respect to a set of field stars for each night. For all differential measurements, we used a very small aperture chosen to maximize the signal-to-noise ratio of the instrumental magnitude. In our data, this maximum occurs for a 5-pixel-radius object aperture. This radius corresponds to 4.8 arcsec and 7 arcsec diameter apertures for the 1.8-m and 1.1-m telescopes, respectively. The seeing was typically about 3 arcsec for all nights but there was some frame-to-frame variation.

We based the absolute calibration for our photometry on data from our best photometric night, 1992 February 24. On that night we observed six different standards from Landolt (1983) and all the asteroid fields from previous nights. An 8-pixel-radius object aperture proved to be sufficient for extracting absolute photometry while avoiding variations caused by seeing. The V filter did have a substantial color term and a weak second order extinction correction but no such corrections were required for the R filter.

The differential photometry in R was simple to reduce. For each field we identified the brightest useful (i.e., nonsaturated) field star as the primary reference. All the other field stars were corrected to have the same mean as the primary field star. We created the final comparison star from an unweighted average of the corrected stars. An unweighted average gave a much better value for the mean as well as a more reliable uncertainty than was the case for a weighted average. The differential photometry for the asteroid on each night was thus its instrumental magnitude minus the composite comparison star magnitude for that image. The uncertainty comes from adding, in quadrature, the uncertainties for the asteroid and the comparison star.

The procedure for reducing the differential V photometry was similar to that for R but was complicated by the presence of the nonzero color terms. Before comparing each star to the primary field star, we applied the second-order extinction and the color term to the instrumental magnitude thus correcting for the color of each field star. This partially transformed magnitude does include the uncertainties on the color term coefficients. The rest of the reductions proceeded in a manner similar to the R data reductions.

To get the data on an absolute system, we added the standard magnitude (as determined on 1992 February 24) of the primary comparison star to the differential photometry. Each night was measured with respect to a different star but we chose to not propagate the uncertainty on the comparison star into the final magnitude at this stage.

Tables II, III, and IV contain the absolute photometry of (5145) Pholus from our reductions. The Julian dates listed are the topocentric midtimes of observation and the magnitudes are apparent V and R. The quality of data presented in Table II is quite good for a 1.1-m telescope, especially considering the conditions. Most data were taken through clouds with extinction as high as 2 mag at times. Such data are identifiable by the increase in σ. The V data in Table III have larger σ primarily because of the uncertainties on the color terms for the V transformation. We tabulate the data from 1992 February 05 separately in Table IV because a different filter was used. We do not have any accurate color transformation for this filter and as such the absolute calibration is more poorly known.

ANALYSIS

Period Determination

We combined all the data in Tables II–IV to establish the rotational period of (5145) Pholus. First, we removed the effect of the changing distance to the asteroid. Using the orbit from MPC 19858, we corrected the data to 1 AU from the Sun and 1 AU from the Earth and applied lighttime correction to do the period analysis in an asteroid-centric reference frame. All effects due to color and solar phase angle remain in the data at this stage.

We determined the best period using the technique of phase dispersion minimization (PDM) based loosely on the procedure described by Stellingwerf (1978). Because

TABLE II
R Photometry of 5145 (1992 AD)

JD	R	σ	JD	R	σ	JD	R	σ
1992 Jan 26			2448653.8876	16.158	0.005	2448674.8101	16.347	0.020
2448647.7447	16.098	0.008	2448653.8930	16.190	0.005	2448674.8137	16.302	0.015
2448647.7486	16.047	0.013	2448653.8967	16.185	0.004	2448674.8174	16.268	0.027
2448647.7522	16.088	0.019	2448653.9004	16.199	0.004	1992 Feb 23		
2448647.7559	16.045	0.025	2448653.9040	16.207	0.004	2448675.6473	16.349	0.015
2448647.7609	16.128	0.043	2448653.9077	16.222	0.004	2448675.6519	16.320	0.020
2448647.7646	15.989	0.020	2448653.9171	16.244	0.005	2448675.6560	16.298	0.017
2448647.7682	16.048	0.010	2448653.9208	16.238	0.007	2448675.6610	16.288	0.022
2448647.7729	16.020	0.010	2448653.9244	16.239	0.005	2448675.6646	16.307	0.007
2448647.7765	16.018	0.005	2448653.9281	16.262	0.007	2448675.6683	16.283	0.010
2448647.7802	16.001	0.006	2448653.9318	16.255	0.005	2448675.6730	16.298	0.008
2448647.7998	15.976	0.005	2448653.9368	16.253	0.008	2448675.6767	16.288	0.007
2448647.8450	16.021	0.004	2448653.9406	16.247	0.007	2448675.6840	16.283	0.012
2448647.8486	16.029	0.005	2448653.9442	16.247	0.007	2448675.7006	16.303	0.010
2448647.8663	16.072	0.007	2448653.9479	16.266	0.011	2448675.7042	16.342	0.010
2448647.8700	16.075	0.004	2448653.9515	16.260	0.009	2448675.7086	16.324	0.012
2448647.8882	16.113	0.008	2448653.9552	16.261	0.006	2448675.7205	16.352	0.018
2448647.8919	16.120	0.009	2448653.9590	16.262	0.008	2448675.7419	16.395	0.012
2448647.8955	16.127	0.009	2448653.9627	16.269	0.007	2448675.7456	16.424	0.011
2448647.9472	16.073	0.012	2448653.9664	16.262	0.013	2448675.7493	16.429	0.008
2448648.0020	15.970	0.020	2448653.9700	16.239	0.013	2448675.7544	16.441	0.007
2448648.0057	15.986	0.019	2448653.9737	16.237	0.011	2448675.7581	16.449	0.012
2448648.0093	15.987	0.030	2448653.9775	16.222	0.010	2448675.7618	16.440	0.006
2448648.0132	16.017	0.034	2448653.9811	16.205	0.015	2448675.7670	16.455	0.008
1992 Feb 01			2448653.9848	16.209	0.011	2448675.7707	16.457	0.011
2448653.7085	16.200	0.007	2448653.9889	16.190	0.007	2448675.7743	16.452	0.011
2448653.7123	16.197	0.004	2448653.9925	16.171	0.007	2448675.7790	16.465	0.012
2448653.7160	16.222	0.006	2448653.9962	16.174	0.006	2448675.7827	16.452	0.008
2448653.7196	16.224	0.004	1992 Feb 22			2448675.7863	16.456	0.009
2448653.7233	16.226	0.008	2448674.6033	16.320	0.008	2448675.7902	16.451	0.010
2448653.7269	16.228	0.007	2448674.6071	16.295	0.008	2448675.7938	16.440	0.008
2448653.7309	16.237	0.007	2448674.6110	16.308	0.008	2448675.7975	16.444	0.009
2448653.7346	16.242	0.005	2448674.6234	16.285	0.008	2448675.8020	16.401	0.014
2448653.7383	16.244	0.008	2448674.6272	16.285	0.010	2448675.8056	16.401	0.012
2448653.7419	16.229	0.005	2448674.6309	16.293	0.005	2448675.8093	16.419	0.014
2448653.7456	16.214	0.004	2448674.6431	16.301	0.006	2448675.8205	16.388	0.009
2448653.7494	16.221	0.004	2448674.6469	16.307	0.006	2448675.8242	16.398	0.009
2448653.7531	16.219	0.004	2448674.6506	16.314	0.007	2448675.8546	16.330	0.011
2448653.7567	16.212	0.004	2448674.6626	16.320	0.007	2448675.8582	16.345	0.011
2448653.7604	16.203	0.005	2448674.6663	16.336	0.009	2448675.8619	16.307	0.009
2448653.7640	16.190	0.005	2448674.6701	16.351	0.007	1992 Feb 24		
2448653.7682	16.190	0.005	2448674.6781	16.355	0.007	2448676.5966	16.435	0.009
2448653.7719	16.172	0.004	2448674.6821	16.363	0.006	2448676.6004	16.454	0.010
2448653.7755	16.161	0.004	2448674.6857	16.371	0.004	2448676.6041	16.460	0.009
2448653.7798	16.167	0.007	2448674.6894	16.382	0.008	2448676.6121	16.456	0.007
2448653.7834	16.149	0.007	2448674.7016	16.400	0.010	2448676.6199	16.452	0.007
2448653.7871	16.157	0.006	2448674.7052	16.419	0.009	2448676.6275	16.450	0.006
2448653.7907	16.139	0.008	2448674.7089	16.434	0.007	2448676.6353	16.428	0.007
2448653.7944	16.138	0.006	2448674.7211	16.462	0.011	2448676.6431	16.422	0.006
2448653.7985	16.130	0.008	2448674.7247	16.464	0.007	2448676.6508	16.401	0.006
2448653.8022	16.116	0.006	2448674.7284	16.451	0.006	2448676.6589	16.386	0.006
2448653.8058	16.106	0.007	2448674.7418	16.460	0.011	2448676.6668	16.363	0.007
2448653.8095	16.111	0.004	2448674.7454	16.445	0.019	2448676.6746	16.355	0.010
2448653.8183	16.087	0.007	2448674.7491	16.491	0.039	2448676.6822	16.335	0.008
2448653.8221	16.090	0.004	2448674.7533	16.477	0.024	2448676.6905	16.330	0.006
2448653.8258	16.086	0.005	2448674.7569	16.492	0.020	2448676.7061	16.319	0.007
2448653.8294	16.095	0.004	2448674.7606	16.458	0.018	2448676.7137	16.316	0.007
2448653.8331	16.068	0.005	2448674.7652	16.461	0.020	2448676.7349	16.339	0.007
2448653.8367	16.085	0.012	2448674.7689	16.468	0.023	2448676.7425	16.361	0.006
2448653.8425	16.090	0.005	2448674.7725	16.424	0.014	2448676.7619	16.390	0.006
2448653.8461	16.103	0.004	2448674.7763	16.437	0.014	2448676.7694	16.396	0.008
2448653.8498	16.086	0.005	2448674.7800	16.415	0.015	2448676.7903	16.448	0.006
2448653.8534	16.098	0.006	2448674.7836	16.402	0.013	2448676.7979	16.444	0.006
2448653.8571	16.101	0.008	2448674.7877	16.400	0.019	2448676.8055	16.452	0.006
2448653.8611	16.102	0.007	2448674.7913	16.382	0.022	2448676.8460	16.471	0.007
2448653.8648	16.112	0.005	2448674.7950	16.340	0.023	2448676.8535	16.466	0.007
2448653.8685	16.118	0.005	2448674.7988	16.412	0.025	2448676.8784	16.364	0.009
2448653.8721	16.110	0.008	2448674.8025	16.401	0.051	2448676.8860	16.365	0.012
2448653.8758	16.131	0.005	2448674.8062	16.265	0.045			

TABLE III
V Photometry of 5145 (1992 AD)

JD	V	σ	JD	V	σ	JD	V	σ
1992 Jan 25			2448674.6936	17.189	0.032	2448676.6630	17.181	0.032
2448646.7428	16.780	0.032	2448674.6972	17.217	0.032	2448676.6707	17.206	0.032
2448646.7608	16.777	0.032	2448674.7132	17.232	0.033	2448676.6784	17.156	0.032
2448646.8821	16.927	0.033	2448674.7168	17.254	0.033	2448676.6862	17.161	0.032
2448646.9041	16.912	0.034	2448674.7333	17.236	0.034	2448676.6942	17.151	0.032
2448647.0035	16.725	0.046	2448674.7370	17.267	0.033	2448676.7022	17.147	0.031
2448647.0074	16.748	0.048	1992 Feb 24			2448676.7099	17.138	0.032
1992 Feb 22			2448676.6079	17.293	0.033	2448676.7386	17.166	0.031
2448674.6151	17.092	0.033	2448676.6160	17.267	0.033	2448676.7657	17.206	0.031
2448674.6191	17.088	0.035	2448676.6237	17.278	0.033	2448676.7942	17.243	0.032
2448674.6354	17.081	0.032	2448676.6313	17.265	0.033	2448676.8018	17.283	0.032
2448674.6391	17.096	0.032	2448676.6392	17.235	0.033	2448676.8498	17.279	0.035
2448674.6546	17.121	0.034	2448676.6469	17.221	0.032	2448676.8822	17.150	0.039
2448674.6583	17.121	0.032	2448676.6550	17.182	0.032			

our data are of varying quality, we modified Stellingwerf's approach to include weighting. Our data consist of three quantities, the asteroid-centric time of observation y_i, distance-corrected magnitude m_i, and the uncertainty for each measurement σ_i. Rather than use the θ-statistic as defined by Stellingwerf, we use χ^2. Similar to Stellingwerf, the data are binned into N_b bins of width δ which usually overlap. The value for the bin width must be set to ensure a "reasonable" number of points in each bin. For this dataset, we chose $\delta = 1/40$ and $N_b = 80$ which resulted in six to nine points per bin. For each bin j, we compute

$$\chi_j^2 = \frac{1}{n_j - 1} \sum_{i=1}^{n_j} \left(\frac{y_i - \overline{y_j}}{\sigma_i} \right)^2, \quad (1)$$

where n_j is the number of points in the bin and $\overline{y_j}$ is the weighted mean of the points in the bin. The weighted mean is computed using statistical weights of $1/\sigma_i^2$. The final statistic computed for each trial period is then

$$\chi^2 = \frac{1}{N_b} \sum_{j=1}^{N_b} \chi_j^2. \quad (2)$$

The advantage of this method is that the uncertainties can be used to compute a weighted statistic that measures the spread of the data within a bin. This is not true of the θ statistic which is based on the variance within a bin. With θ, the weights lead to a weighted mean but the variance of the bin does not depend on the true spread in the data in cases where the distribution is not normal (ie., the wrong period). As with θ, the minimum of χ^2 determines the best rotational period. If the uncertainties on the measurements are correct, then χ^2 at the correct period should be unity. At the wrong period, there is no upper limit to χ^2. However, the range of χ^2 one finds in searching for a

TABLE IV
Additional R^* Photometry of 5145 (1992 AD)

JD	R*	σ	JD	R*	σ	JD	R*	σ
1992 Feb 05			2448657.8369	16.111	0.009	2448657.9193	16.186	0.005
2448657.6050	16.079	0.013	2448657.8395	16.113	0.004	2448657.9360	16.162	0.009
2448657.6070	16.126	0.011	2448657.8422	16.125	0.004	2448657.9386	16.164	0.006
2448657.6201	16.132	0.004	2448657.8449	16.127	0.004	2448657.9413	16.156	0.007
2448657.6220	16.146	0.005	2448657.8619	16.163	0.007	2448657.9440	16.152	0.006
2448657.6506	16.189	0.005	2448657.8653	16.152	0.007	2448657.9621	16.104	0.006
2448657.6526	16.200	0.006	2448657.8679	16.176	0.005	2448657.9649	16.109	0.008
2448657.7822	16.063	0.005	2448657.8705	16.185	0.004	2448657.9675	16.085	0.008
2448657.7848	16.060	0.005	2448657.8888	16.212	0.010	2448657.9713	16.086	0.009
2448657.7874	16.063	0.006	2448657.8914	16.218	0.005	2448657.9739	16.067	0.011
2448657.8050	16.063	0.007	2448657.8945	16.214	0.006	2448657.9784	16.075	0.020
2448657.8076	16.054	0.008	2448657.8971	16.229	0.004	2448657.9819	16.062	0.014
2448657.8111	16.102	0.011	2448657.9141	16.211	0.005	2448657.9845	16.071	0.010
2448657.8191	16.091	0.011	2448657.9167	16.209	0.006	2448657.9872	16.065	0.020

period gives a very good indication of the significance of the rotational modulation of the lightcurve.

Before extracting the period from the data, we removed the relative shifts between nights caused by using different filters and the changing solar phase angle. To determine these shifts we used another variant on phase dispersion minimization. This time we minimized χ^2 with respect to the vertical shift of the data. In computing the shift, we always compared two nights at a time using the lightcurve on 1992 February 01 as the primary reference lightcurve.

Determining the period and relative shifts is an iterative process. In general, one must determine the optimum set of shifts for each trial period. In practice, this is not necessary since the overall behavior of χ^2 with period is only weakly dependent on the shifts. We found the best fit period by alternately determining the shifts while holding the period fixed and then improving the period while holding the shifts constant. The process converged after just a few iterations.

Once we were close to a period we defined UT 1992 January 23 21 : 00 : 00 to be the asteroid-centric reference epoch from which to measure the rotational phase. This reference time was chosen to coincide with the sharper of the two lightcurve minima. The other minimum is actually deeper but is less well defined in our dataset.

We examined a broad range of rotational periods looking for the best fit period. The deepest minimum of χ^2 was at a period of 9.9825 ± 0.0040 hr and compares very well with our initial determination (Buie *et al.* 1992). This period corresponds to the double-peaked lightcurve typical of most asteroids. We found no evidence for a period near 13.2 hr as suggested by Hoffman *et al.* (1992).

We constrained the uncertainty on the period by using the point on the χ^2 versus period curve that is 50% larger than the minimum for the optimum period. When applied to our data, this criterion corresponds to the change in period allowed before the combined lightcurve begins to look poorly phased. The best-fit period may be even better determined than we indicate, but it is certainly not worse.

Plotted in Fig. 1 are the data from Tables II–IV shown against the rotational phase from the best-fit period. The solid curve overlaid on each night's data is from a high-order Legendre polynomial fit to all of the data and provides a constant visual reference. There is no evidence in our data for any significant evolution of the lightcurve over the time span of our observations. In Fig. 2 we have plotted all the data on the same scale. From this lightcurve we see that the minima occur almost exactly at 0.0 and 0.5 rotational phase. The maxima are also spaced by half of a rotation but occur near rotational phases 0.2 and 0.7, rather than 0.25 and 0.75. The maxima are clearly seen to be of almost equal brightness while the minima differ by 0.04 mag. Because of the present lack of aspect information on (5145) Pholus, we have not attempted to infer any shape information.

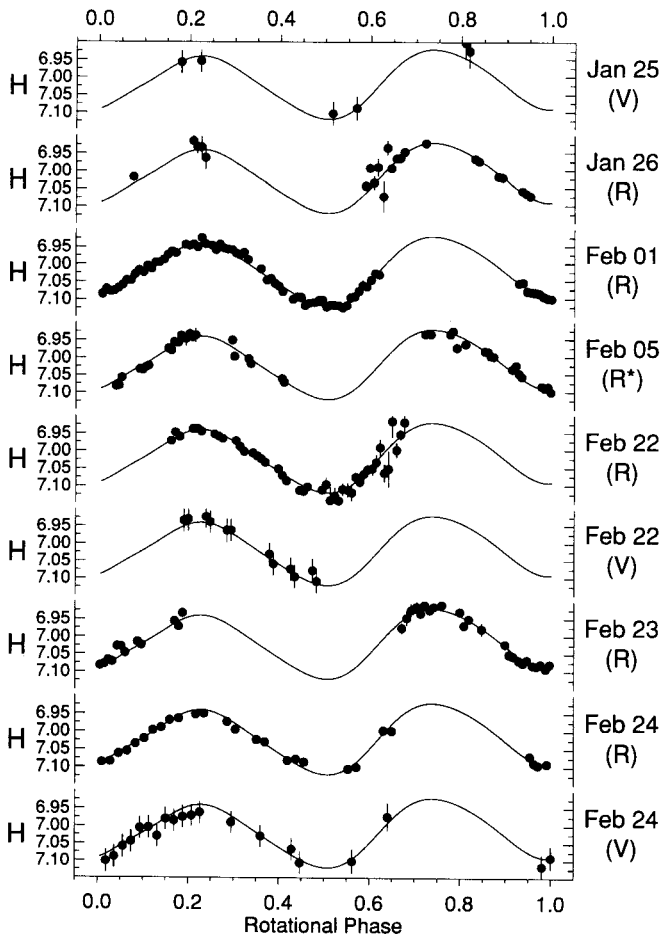

FIG. 1. This figure shows all the photometry from Tables II–IV for (5145) Pholus. All data have been corrected to 1 AU from the Sun, 1 AU from the Earth, zero degree phase angle, and R magnitude, that is, the standard H_R value from the IAU standard two parameter fit. The solid curve is from a Legendre polynomial fit to all the data and is plotted as a visual aid.

V-R Color

Our determination of the $(V - R)$ color of (5145) Pholus derives from the two-color data on 1992 February 22 and 24. In every case, a pair of R measurements straddles each V measurement. We interpolated the R magnitude to match the time of each V measurement using the two nearest R points. From the interpolated measurements we thus have a set of $(V - R)$ points. Our measurements, shown in Fig. 3, constrain the amplitude of any color variation to be less than 0.04 mag. Averaging all the points results in a "globally" averaged value of $(V - R) = 0.810 \pm 0.006$.

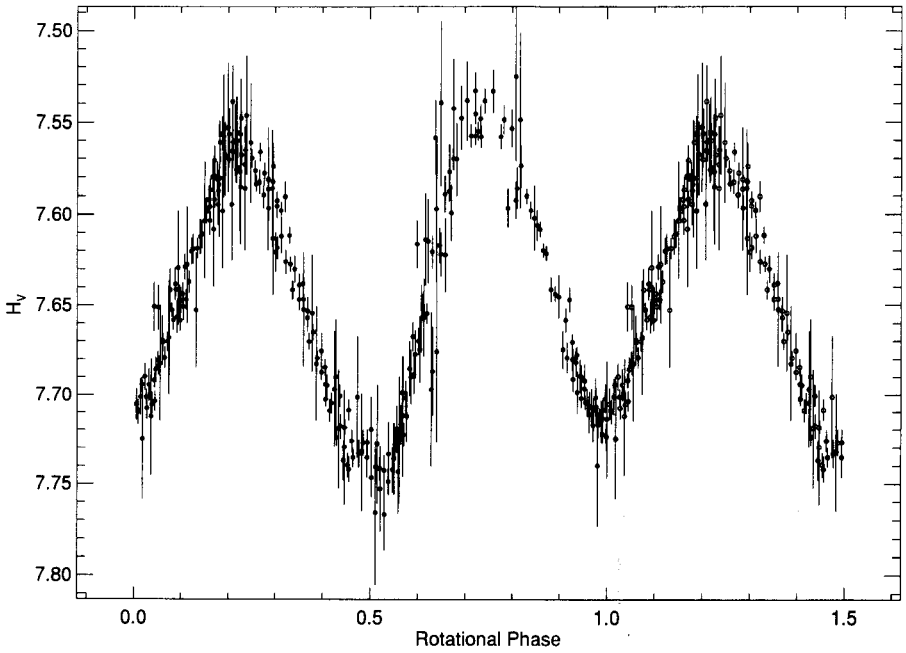

FIG. 2. Composite lightcurve for (5145) Pholus. All measurements (corrected to V) from Fig. 1 are shown overlaid on the same scale.

H and G Parameter Fit

To facilitate a comparison of our photometry with other asteroids we modeled our photometry as a function of solar phase angle with a least squares fit to the IAU standard two parameter system (Bowell *et al.* 1989). Figure 4 shows the lightcurve mean for each night plotted against the solar phase angle. The solid curve is the fitted curve for $H_V = 7.645 \pm 0.011$ and $G_V = 0.16 \pm 0.08$. We omitted the photometry from 1992 February 05 in this determination since its transformation to an absolute magnitude was too uncertain. These H and G values are very typical for asteroids in general despite the very unusual color. The range of phase angles is restricted for (5145) Pholus and limits the usefulness of the number. However, we can rule out strong opposition surges that are wider than 0.5°.

DISCUSSION

Except for the $(V - R)$ color, all the physical observations presented in this work are very normal values for asteroids in general. When plotted with asteroids with known H and G values, (5145) Pholus plots in the middle of the distribution. Most values that have been determined are for particularly well studied objects and are quite typical of main-belt asteroids. Similarly, the lightcurve properties (period and amplitude) are not unusual.

If one were allowed to ignore the color of this object,

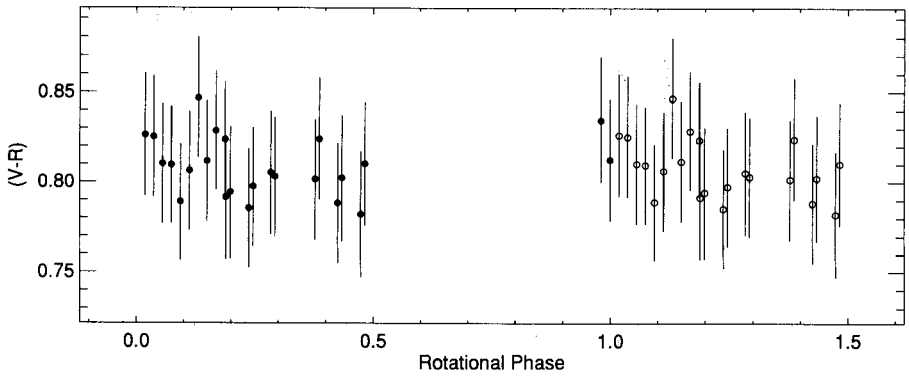

FIG. 3. $(V - R)$ color for (5145) Pholus versus rotational phase. No significant color variations can be seen. All of these color measurements were made at nearly the same solar phase angle.

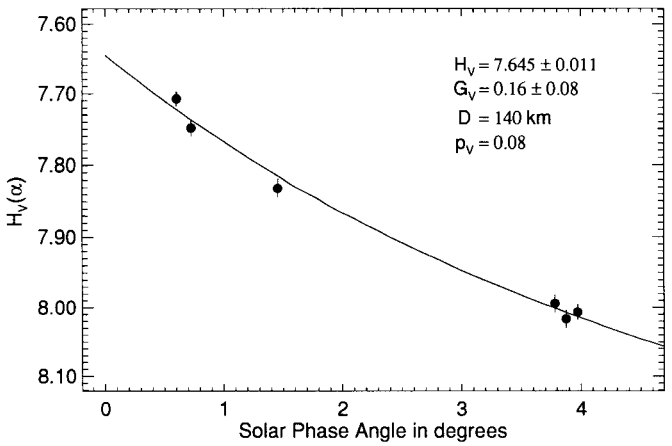

FIG. 4. Solar phase angle data for (5145) Pholus. The solid points are the mean magnitudes from each night corrected to standard distance and corrected to V. The solid line is from the H_V and G_V fit to the data. The diameter shown is the value reported by Howell *et al.* (1992) and the geometric albedo is derived from this diameter using our photometry.

one might easily conclude that (5145) Pholus was perturbed out of the main belt and perhaps is in a dynamically young or unstable orbit. Further study into the orbital evolution may yet yield such a conclusion. Clearly the present orbit is very unusual for known asteroids and the question remains about the total population of objects with orbits similar to (5145) Pholus and (2060) Chiron.

However, we cannot ignore the unusual color nor its invariance with rotational phase. Whatever the source of the color, the reddening agent must be global. Both Fink *et al.* (1992) and Mueller *et al.* (1992) suggest that the color may be due to some type of organic residues and this is certainly a reasonable hypothesis given what we now know from laboratory studies. However, the spectrum shown by Fink *et al.* is truly remarkable in its lack of any spectral variations other than a linear slope. Such is not the case for the laboratory materials shown (in particular, the UV tholin and the spark tholin). All currently published spectra of extreme red substances contain some inflection points across this spectral region. While we agree that organic residues are a likely candidate, there is still too little laboratory data on the spectral properties of residues with time, total irradiation dosage, and composition to permit a definitive comparison. Also, we still know nothing about the particulate nature of these materials in an environment found on the surface of (5145) Pholus. Modeling of the scattering properties as well as of the spectral properties will be required for complete understanding of this unique object.

ACKNOWLEDGMENTS

This research was made possible by funds from the Lowell Observatory Endowment and also from NASA Grant NAGW-1470. Thanks also go to Brian Skiff for assisting with the observations.

REFERENCES

BOWELL, E., B. HAPKE, D. DOMINGUE, K. LUMME, J. PELTONIEMI, AND A. W. HARRIS 1989. Application of photometric models to asteroids. In *Asteroids II* (R. P. Binzel, T. Gehrels, and M. S. Matthews, Eds.), pp. 549–554. Univ. of Arizona Press, Tucson.

BUIE, M. W., S. J. BUS, AND B. A. SKIFF 1992. *1992 AD.* IAU Circular 5451.

DAVIES, J. K. AND M. V. SYKES 1992. *(5145) 1992 AD.* IAU Circular 5480.

FINK, U., M. HOFFMAN, W. GRUNDY, M. HICKS, AND W. SEARS 1992. The steep red spectrum of *1992 AD*: An asteroid covered with organic material? *Icarus* **97,** 145–149.

HAHN, G., AND M. E. BAILEY 1990. Rapid dynamical evolution of giant comet Chiron. *Nature* **348,** 132–136.

HAINAUT, O., AND A. SMETTE 1992. *1992 AD.* IAU Circular 5450.

HOFFMAN, M., U. FINK, W. GRUNDY, AND M. HICKS 1992. IAU Circular 5458.

HOWELL, E., R. MARCIALIS, R. CUTRI, M. NOLAN, L. LEBOFSKY, AND M. SYKES 1992. IAU Circular 5449.

KHARE, B. N., C. SAGAN, J. ZUMBERGE, D. SKLAREW, AND B. NAGY 1981. Organic solids produced by electrical discharge in reducing atmospheres: Tholin molecular analysis. *Icarus* **48,** 290–297.

KOWAL, C. T., W. LILLER, AND B. G. MARSDEN 1979. The discovery and orbit of (2060) Chiron. In *Dynamics of the Solar System* (R. L. Duncombe, Ed.), pp. 245–250. Reidel, Boston.

LANDOLT, A. U. 1983. UBVRI photometric standard stars around the celestial equator. *Astron. J.* **88,** 439–460.

MUELLER, B. E. A., D. J. THOLEN, W. K. HARTMANN, AND D. P. CRUIKSHANK 1992. Extraordinary colors of asteroidal object (5145) 1992 AD. *Icarus* **97,** 150–154.

OIKAWA, S., AND E. EVERHART 1979. Past and future orbit of 1977 UB, object Chiron. *Astron. J.* **84,** 134–139.

PRESS, W. H., B. P. FLANNERY, S. A. TEUKOLSKY, AND W. T. VETTERLING 1988. *Numerical Recipes in C,* Section 13.1, pp. 472–476. Cambridge Univ. Press, Cambridge.

SCHOLL, H. 1979. History and evolution of Chiron's orbit. *Icarus* **40,** 345–349.

SCOTTI, J. V. 1992. *1992 AD.* IAU Circular 5434.

SPENCER, J. R., L. A. LEBOFSKY, AND M. V. SYKES 1989. Systematic biases in radiometric diameter determinations. *Icarus* **78,** 337–354.

STELLINGWERF, R. F. 1978. Period determination using phase dispersion minimization. *Astrophys. J.* **224,** 953–960.

STRAZZULLA, G., L. CALCAGNO, AND G. FOTI 1984. Build up of carbonaceous material by fast protons on Pluto and Triton. *Astron. Astrophys.* **140,** 441–444.

WILLIAMS, G. V. 1992a. IAU Circular 5435.

WILLIAMS, G. V. 1992b. Minor Planet Circular 19850.